

**Supplemental information for  
Design and performance evaluation of a PN<sub>1</sub> sensor for real-time  
measurement of indoor aerosol size distribution**

**Junho Hyun<sup>1</sup>, Jangseop Han<sup>2</sup>, Sang-Gu Lee<sup>1</sup>, Jungho Hwang<sup>1,2\*</sup>**

<sup>1</sup> *Graduate program of Clean Technology, Yonsei University,  
50 Yonsei-ro, Seodaemun-gu, Seoul, Korea.*

<sup>2</sup> *Department of Mechanical Engineering, Yonsei University,  
50 Yonsei-ro, Seodaemun-gu, Seoul, Korea*

---

\* Corresponding author. Tel: 82-2-2123-2821; Fax: 82-2-312-2821  
E-mail address: hwangjh@yonsei.ac.kr

## INFORMATION AVAILABLE

This section provides the following information:

1. Geometrical design parameters for impactor and boundary conditions for numerical calculation;
2. Charging theories;
3. Performance test of Faraday cage;
4. Performance test of lab-made electrometer;
5. Size distribution of ambient aerosols.

### **1. Geometrical design parameters for impactor+ and boundary conditions for numerical calculation**

Figure S1 shows the geometrical design parameters for the impactor. For boundary #1 (inflow boundary), the pressure is set to standard atmospheric pressure. For boundary #2 (major flow boundary), the velocity is set in the x direction. For boundary #3 (minor flow boundary), the velocity is set in the  $-y$  direction. Boundary #4 (wall boundary) uses the no-slip flow and particle trap conditions. Boundary #5 uses the symmetric conditions. The diameters  $L_{\text{inlet}}$ ,  $L_{\text{major}}$ , and  $L_{\text{minor}}$  are all 6.3 mm.

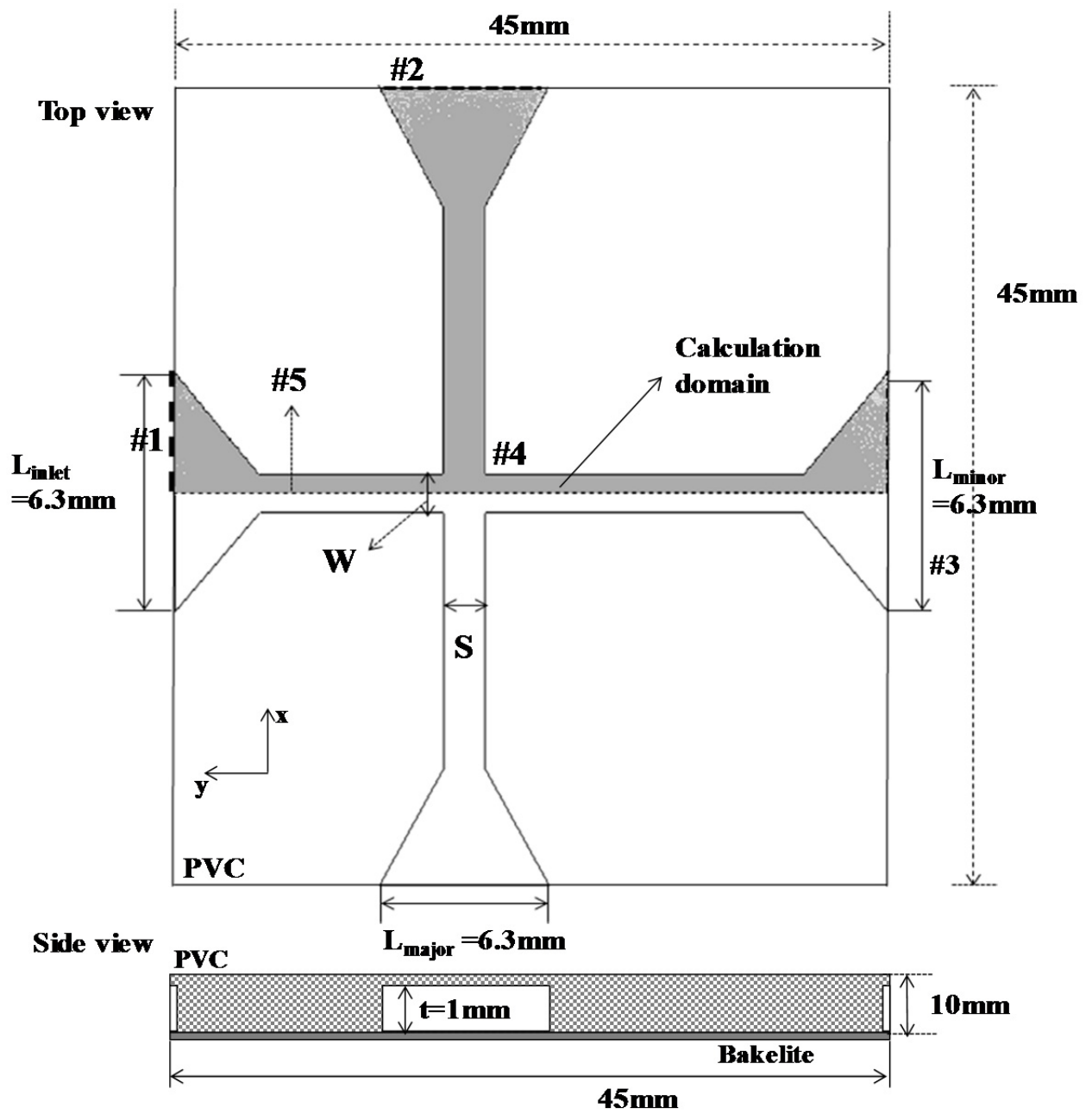


Fig. S1 Geometrical design parameters for virtual impactor.

## 2. Charging theories

The experimentally determined particle charge is compared with the charge  $n_c$  calculated from the sum of the diffusion ( $n_d$ ) and field ( $n_f$ ) charging theories:

$$n_c(d_p) = n_d(d_p) + n_f(d_p) \quad (\text{S1})$$

where

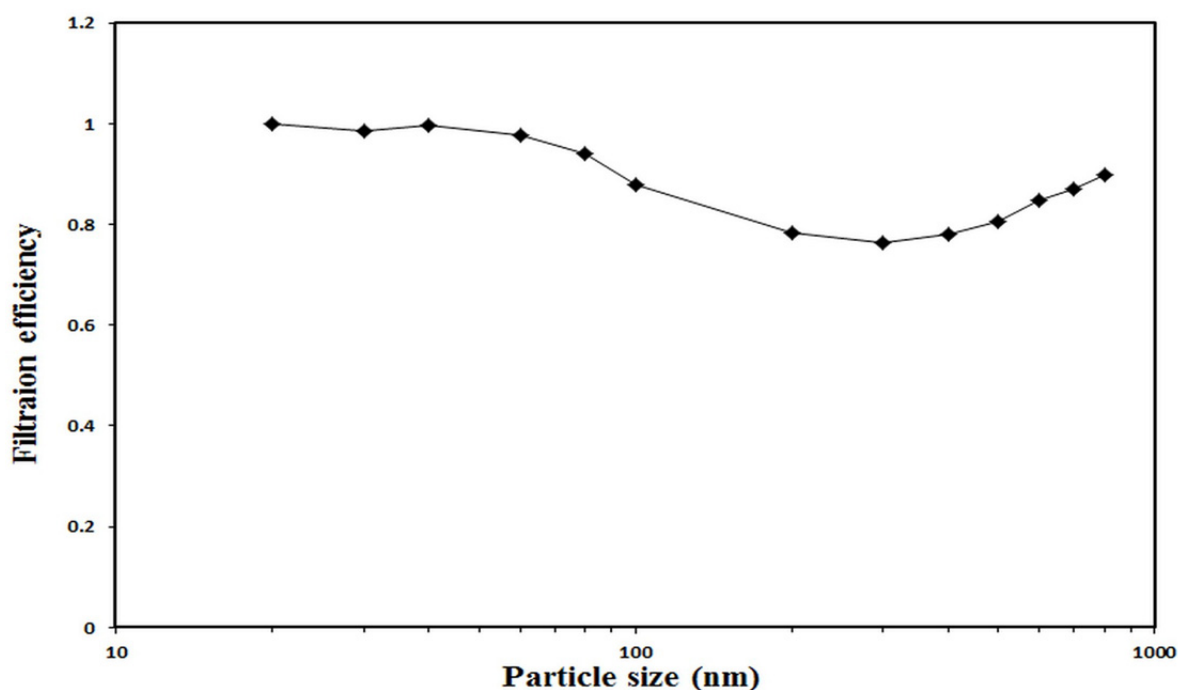
$$n_d(d_p) = \frac{d_p kT}{2K_E e^2} \ln \left[ 1 + \frac{\pi K_E d_p \bar{c}_i e^2 N_i t}{2kT} \right] \quad (\text{S2})$$

$$n_f(d_p) = \left( \frac{3\varepsilon}{\varepsilon + 2} \right) \left( \frac{Ed^2}{4K_E e} \right) \left( \frac{\pi K_E e Z_i N_i t}{1 + \pi K_E e Z_i N_i t} \right) \quad (\text{S3})$$

In Eqs. (S2) and (S3),  $k$  is the Boltzmann constant,  $T$  is the absolute temperature,  $\bar{c}_i$  is the mean velocity of air ion (240 m/s),  $\varepsilon$  is the relative permittivity of a particle,  $K_E$  is a constant of proportionality, and  $t$  is the residence time in the charger.

### 3. Performance of Faraday cage

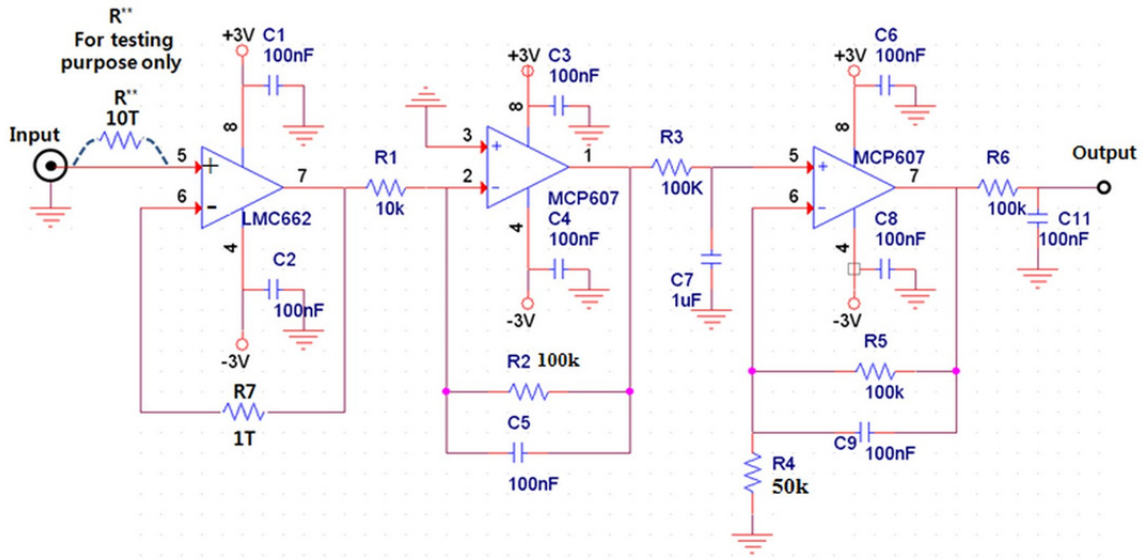
Figure S2 shows the filtration efficiencies of the metal filter for various particle sizes. The particle size that gives the minimum efficiency (0.3  $\mu\text{m}$ ) is an intermediate size that is too large for diffusion to be effective and too small for impaction or interception to be effective. Because these competing mechanisms are most effective in different size ranges, all filters have a particle size that gives minimal efficiency, usually in the range 0.05–0.5  $\mu\text{m}$ . For 0.3  $\mu\text{m}$  particles, the minimum efficiency is 77%.



**Fig. S2 Filtration efficiency of Faraday cage (standard deviation for each datum ~ 5%).**

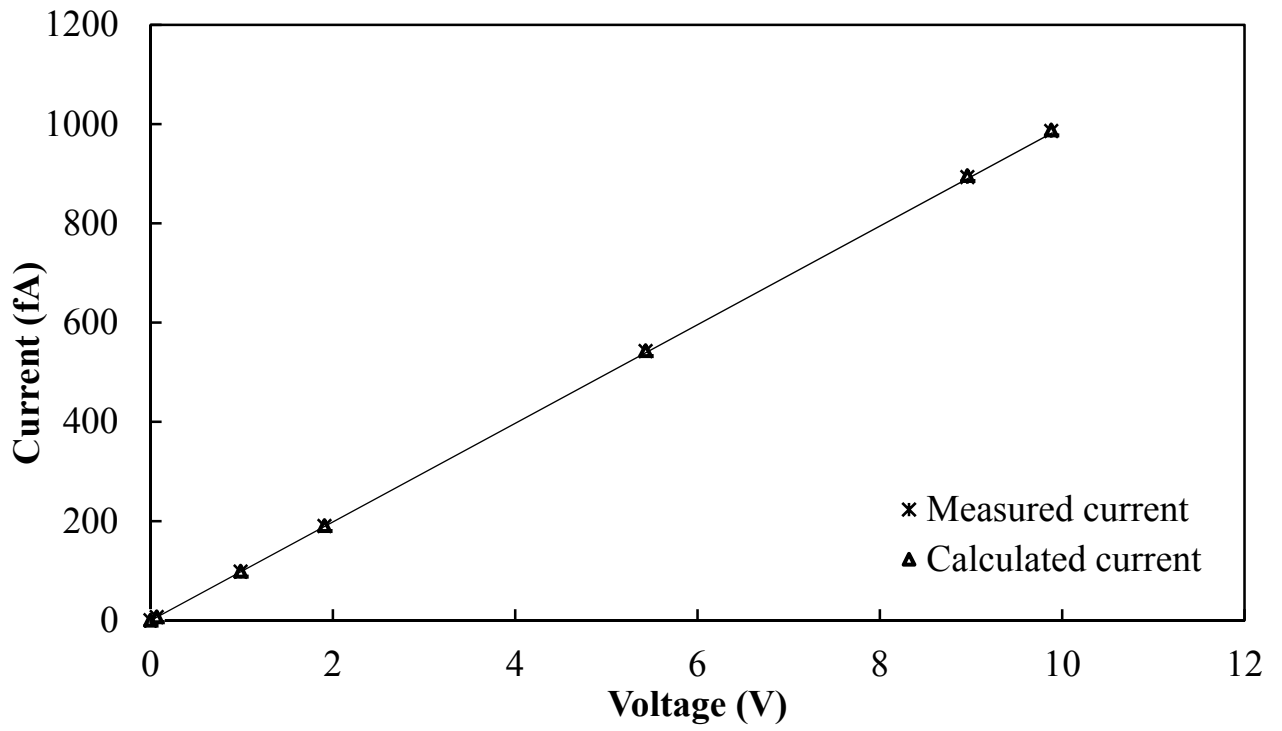
#### **4. Performance of lab-made electrometer**

Figure S3 shows a circuit diagram of the electrometer. We used a three-stage amplifier circuit to obtain a stable output signal with a total amplification rate of  $1.69 \times 10^{12}$  V/A: (first) current-to-voltage converter, (second) inverting amplifier, (third) noninverting amplifier. The feedback capacitors (C5, C9) and RC low-pass filters (R3 and C7, R6 and C11) reduce high-frequency noise and prevent the amplifier output from oscillating. Also, a power-supply filtering scheme is adopted in the amplifier power rails by adding 100 nF capacitors. Commercially available low-cost high-impedance operational amplifiers are used: LMC662 featuring ultralow input bias current (2 fA maximum) and low-offset voltage drift ( $1.3 \mu\text{V}/^\circ\text{C}$ ).



**Fig. S3 Circuit diagram of electrometer.**

A DC voltage signal from a power supply is applied to the input of the amplifier via a  $10\text{ T}\Omega$  resistor (see Figure S3). The output signal processed through the microprocessor is displayed on the LCD panel of the electrometer. Subsequently, this displayed value is compared with the current calculated by applying Ohm's law to the  $10\text{ T}\Omega$  resistor. Figure S4 shows that the correlation coefficient between the displayed value and the calculated current is almost 100%.



**Fig. S4 Comparison of current measured by electrometer with calculated current (standard deviation for each datum ~ 1%).**